

RESEARCH

Open Access



Non-additive expression genes play a critical role in leaf vein ratio heterosis in *Nicotiana tabacum* L.

Lili Duan^{1,2,3}, Zejun Mo^{1,2}, Kuiyin Li⁴, Kai Pi^{1,2,3}, Jiajun Luo^{1,2}, Yuanhui Que¹, Qian Zhang^{1,2}, Jingyao Zhang¹, Guizhi Wu¹ and Renxiang Liu^{1,2*}

Abstract

Heterosis, recognized for improving crop performance, especially in the first filial (F_1) generation, remains an area of significant study in the tobacco industry. The low utilization of leaf veins in tobacco contributes to economic inefficiency and resource waste. Despite the positive impacts of heterosis on crop genetics, investigations into leaf-vein ratio heterosis in tobacco have been lacking. Understanding the mechanisms underlying negative heterosis in leaf vein ratio at the molecular level is crucial for advancing low vein ratio leaf breeding research. This study involved 12 hybrid combinations and their parental lines to explore heterosis associated with leaf vein ratios. The hybrids displayed diverse patterns of positive or negative leaf vein ratio heterosis across different developmental stages. Notably, the F_1 hybrid (G70 × Qinggeng) consistently exhibited substantial negative heterosis, reaching a maximum of -19.79% 80 days after transplanting. A comparative transcriptome analysis revealed that a significant proportion of differentially expressed genes (DEGs), approximately 39.04% and 23.73%, exhibited dominant and over-dominant expression patterns, respectively. These findings highlight the critical role of non-additive gene expression, particularly the dominance pattern, in governing leaf vein ratio heterosis. The non-additive genes, largely associated with various GO terms such as response to abiotic stimuli, galactose metabolic process, plant-type cell wall organization, auxin-activated signaling pathway, hydrolase activity, and UDP-glycosyltransferase activity, were identified. Furthermore, KEGG enrichment analysis unveiled their involvement in phenylpropanoid biosynthesis, galactose metabolism, plant hormone signal transduction, glutathione metabolism, MAPK signaling pathway, starch, and sucrose metabolism. Among the non-additive genes, we identified some genes related to leaf development, leaf size, leaf senescence, and cell wall extensibility that showed significantly lower expression in F_1 than in its parents. These results indicate that the non-additive expression of genes plays a key role in the heterosis of the leaf vein ratio in tobacco. This study marks the first exploration into the molecular mechanisms governing leaf vein ratio heterosis at the transcriptome level. These findings significantly contribute to understanding leaf vein ratios in tobacco breeding strategies.

Keywords Leaf vein ratio, Heterosis, *Nicotiana tabacum* L., Non-additive, Transcriptomics

*Correspondence:

Renxiang Liu
rxliu@gzu.edu.cn

¹ College of Tobacco, Guizhou University, Guiyang 550025, China

² Key Laboratory for Tobacco Quality Research Guizhou Province, Guizhou University, Guiyang 550025, China

³ College of Agriculture, Guizhou University, Guiyang 550025, China

⁴ Anshun University, Anshun 561099, China

Background

Hybrid vigor, also known as heterosis, refers to the phenomenon where the first-generation offspring (F_1) demonstrates superior agronomic traits compared to its homozygous parents in plants. These enhanced traits often include larger plant stature, increased biomass, growth rate, improved grain yield, quality factors, and



© The Author(s) 2024. **Open Access** This article is licensed under a Creative Commons Attribution-NonCommercial-NoDerivatives 4.0 International License, which permits any non-commercial use, sharing, distribution and reproduction in any medium or format, as long as you give appropriate credit to the original author(s) and the source, provide a link to the Creative Commons licence, and indicate if you modified the licensed material. You do not have permission under this licence to share adapted material derived from this article or parts of it. The images or other third party material in this article are included in the article's Creative Commons licence, unless indicated otherwise in a credit line to the material. If material is not included in the article's Creative Commons licence and your intended use is not permitted by statutory regulation or exceeds the permitted use, you will need to obtain permission directly from the copyright holder. To view a copy of this licence, visit <http://creativecommons.org/licenses/by-nc-nd/4.0/>.

heightened resistance to abiotic stress [1–3]. Heterosis is a widely observed biological phenomenon that significantly benefits crop growth and adaptation to varying environmental conditions [4–6]. At present, there are three competing, but not mutually exclusive, hypotheses to explain the molecular mechanism of heterosis at the genetic level: the dominant hypothesis [7, 8], the superdominant hypothesis [5], and the epistasis hypothesis [9, 10]. Research on heterosis has progressed in various crops [11–14], especially rice and maize [15–20]. Nevertheless, only a limited number of these factors have been systematically characterized for their involvement in yield heterosis [21]. Theoretical research on heterosis lags far behind practical applications and the relative contributions of genetic components vary with different traits and crops [22, 23]. However, there is no consensus on the mechanism of heterosis.

With the advancement of next-generation sequencing technologies, an increasing number of researchers have employed omics technologies to investigate the molecular mechanisms underlying heterosis [24]. In the case of rice, a total of 1.2 Tb of genome sequence was acquired by sequencing 1495 diverse varieties with a two-fold genome coverage [22]. Liu et al. [25], 628 loci with relatively high mapping resolutions were identified from three maize hybrids, revealing that most loci exhibited dominance or overdominance effects on heterosis. Using RNA-seq, 75,281 genes were obtained from the roots of rapeseed seedling classes. Subsequent analysis highlighted the crucial role of overexpressed differentially expressed genes (DEGs) in hybrid root growth in rapeseed [3]. Another investigation on Chinese cabbage heterosis through transcriptome sequencing demonstrated that over 81% of the DEGs displayed dominant inheritance [13]. In a study, Shahzad et al. [26] focused on yield heterosis in upland cotton, most DEGs in the hybrids exhibited dominant parent expression levels across different tissues, as revealed by comparative transcriptome analysis. Additionally, an examination of Easter lily involved identifying 4,327 DEGs from hybrids and their parents using RNA-Seq [27]. Transcriptomic analysis has proven to be both feasible and reliable in exploring heterosis. However, to date, there have been no reports on the analysis of leaf vein ratio heterosis using omics.

The vein ratio of tobacco leaves denotes the weight percentage of tobacco veins in the leaves [28], serving as a crucial measure for assessing the utility of tobacco leaves. High vein ratios in tobacco leaves result in lower rates of flake and silk production during threshing and redrying, leading to reduced leaf availability. The coarse tobacco veins, often treated as by-products in the cigarette industry, are commonly considered waste, contributing to both resource wastage and environmental pollution,

significantly impacting cigarette processing quality, procurement expenses, and overall profitability [29, 30]. Previous investigations on the vein ratio of tobacco leaves have indicated its hereditary control with high heritability, along with substantial heterosis [31, 32].

Leaves serve as the primary location for plant photosynthesis and are linked to crop productivity [33]. Leaf veins are essential for the transportation of water and nutrients, as well as providing structural support for leaves as they grow and develop [34]. Plant hormones, such as Auxin, gibberellin (GA), and other compounds, are vital in the regulation of leaf growth and development [12, 35]. Auxin plays a crucial role as a signaling molecule necessary for the differentiation and growth of plant leaves. It significantly influences the development of leaf veins through a channelized model of vein formation [36–39]. Currently, numerous studies have identified several genes that play a role in regulating the development of leaf veins. Among these, the *homeodomain-leucine zipper III (HD-ZIP III)* gene has been recognized as a crucial factor in plant leaf vein development. In Arabidopsis, five key *HD-ZIP III* genes, *PHABULOSA (PHB)*, *PHAVOLUTA (REV)*, *CORONA (CNA)*, *ATHB15*, and *ATHB8*, are known to be involved in this process [40]. Apart from the *HD-ZIP III* genes, the *VND* gene family, *SND1* gene family, and MYB transcription factor family play a role in regulating the differentiation and development of vascular bundle tissue [41]. The overexpression of *MYB33* and *MYB65* genes results in the development of phenotypic features of curled leaves and shortened petioles [42]. Xylan transglycosidase/hydrolase (*XTH*) plays a crucial role as a cell wall modifying enzyme during plant cell wall remodeling [43]. *XTH* genes are involved in the regulation of the growth and development in plant leaves [44]. The lack of the *AtXTH27* gene leads to a reduction in the length of third-level branches in rose leaves, and as well as a decrease in the quantity of third-level branches in the initial leaf [45].

Nicotiana tabacum L. ($2n=4x=48$) represents a typical allotetraploid crop derived from the hybridization of *Nicotiana sylvestris* and *Nicotiana tomentosiformis* [33]. Tobacco, a significant cash crop, is cultivated in over 120 countries worldwide [34–37]. Apart from *Arabidopsis thaliana*, tobacco is frequently utilized as a model plant in biological research due to its short growth cycle, susceptibility to diseases, ease of genetic modification, and other favorable attributes [38]. Both inter- and intraspecific tobacco varieties exhibit substantial heterosis [39, 40]. In China, exploration of tobacco heterosis commenced in the 1950s [41, 42]. Research on tobacco heterosis has primarily focused on potassium content [43], root growth [44], leaf area [45], leaf number [46], and nicotine content [47], but advancements have been gradual.

Nonetheless, the molecular foundation underlying leaf vein ratio heterosis in tobacco at the transcriptomic level remains unexplored. This study aims to unravel the mechanism of heterosis formation at the transcriptome level, offering significant practical implications for enhancing the efficiency of leaf vein ratios in hybrid varieties. Furthermore, these findings provide technical guidance and molecular insights to unveil the genetic basis of crop heterosis.

Results

Heterosis performance of vein ratio of leaves in F_1 hybrids

The middle leaves of tobacco typically ripen around 3 weeks after topping. Among the 12 hybrid combinations, consistent heterosis in the leaf vein ratio was observed both 1 week (80 days) and 3 weeks (94 days) after topping. Notably, 50% of combinations exhibited negative heterosis one week after topping (Additional File 1), pinpointing this duration as a pivotal period for leaf vein ratio heterosis formation. The 13 parental materials displayed significant variations in the leaf vein ratio, ranging from 9.70% to 18.23% after 80 days post-transplanting (Fig. 1a). This variation among genotypes underscored ample genetic diversity for enhancing the leaf vein ratio. Among the 12 hybrid combinations, the G70×Qinggeng hybrid consistently demonstrated stable negative heterosis, reaching a maximum of -19.79% after 80 d post-transplanting (Fig. 1b). The leaf vein ratio in G70×Qinggeng measured 9.93%, lower than that of its parents and notably different from the maternal plant after 80 d post-transplanting (Fig. 1c). Additionally, heterosis values categorized as over high parental heterosis (OPH), medium parental heterosis (MPH), and low parental heterosis (BPH) in G70×Qinggeng were -30.58%, -19.79%, and -7.72%, respectively (Fig. 1d). At the same time, the average values of repeated MPH, OPH, and BPH for the hybrid combination G70×Qinggeng in 2020 and 2021 were -16.13%, -28.14%, and -1.96%, respectively (Additional file 2), indicating a substantial infection ability for leaf vein ratio heterosis in hybrid offspring. To delve deeper into the mechanisms underlying leaf vein ratio heterosis, fresh leaf samples from G70×Qinggeng and its parental plants were selected 80 d post-transplanting for transcriptome sequencing analysis. The fresh leaves figure of the hybrid G70×Qinggeng and its parents were shown in Fig. 2.

RNA-seq data analysis of leaves between parents and F_1

In this investigation, we utilized G70×Qinggeng and its parental lines to generate nine cDNA libraries that were subsequently sequenced using an Illumina HiSeq 2000 platform. The quality assessment of sequencing data for the nine cDNA libraries is detailed in Additional File

3. The average error rate across all samples was 0.02%, with Q20 scores exceeding 98.00%, Q30 scores surpassing 94.00%, and GC content measuring above 42.00%. The read and mapping outcomes are displayed in Additional File 4, demonstrating read counts ranging from 68,195,482 to 83,395,016. Over 95.15% of the total sequences were successfully mapped onto the reference genome 'K326', affirming the reliability of the transcriptome sequencing data for subsequent analyses.

For validation purposes, we selected eight genes randomly from the transcriptome results and subjected them to Real-Time Fluorescence Quantitative PCR (qRT-PCR) analysis. Actin served as the internal reference gene to normalize the expression levels of each gene. The genes and corresponding primers employed for qRT-PCR are delineated in Additional File 5. Our findings revealed a consistency between the qRT-PCR expression pattern and the RNA-seq data, affirming the reliability of the transcriptome mapping data (Fig. 3, Additional File 6). These results lay the foundation for subsequent steps in differential gene screening and expression analysis.

DESeq2 software was used to determine the DEGs between the F_1 hybrids and their parents to explore the differences in the expression characteristics of leaf vein ratio heterosis at the transcriptome level. When the parameters were set to $P \leq 0.05$ and $|\log_2 \text{Fold Change}| \geq 2$, 3767 DEGs were identified (Fig. 4). Between the two parents, G70 and Qinggeng, there were 2143 DEGs were identified, including 1121 genes that were up-regulated and 1022 genes that were down-regulated. There were 661 DEGs in the comparison group of ' F_1 vs P1', 322 were up-regulated and 339 were down-regulated. Similarly, there were 824 DEGs between ' F_1 vs P2' (Fig. 4a). Among the 824 DEGs, 382 were upregulated and 442 were downregulated. Common genes among the three groups are shown in Fig. 4b. The venn diagram analysis revealed that the comparison group ' $P1$ vs $P2$ ' and the comparison group ' F_1 vs $P2$ ' share the largest number of genes, which is 444. However, only 58 differential genes shared between the two comparison groups ' F_1 vs $P1$ ' and ' F_1 vs $P2$ '. Furthermore, 108 common differential identified among the three comparison groups.

F_1 hybrid demonstrated a non-additive gene expression pattern

For further analysis of DEGs and to explore the heterosis formation mechanism of the leaf vein ratio in tobacco leaves, 1319 common DEGs were identified between F_1 and the parents (Additional File 7). The 1319 DEGs were divided into 12 expression patterns (P1–P12, Fig. 5a), according to a previously described method [48]. The genes in P1 and P2 were classified as having additive expression patterns. The P3–P6 expression patterns

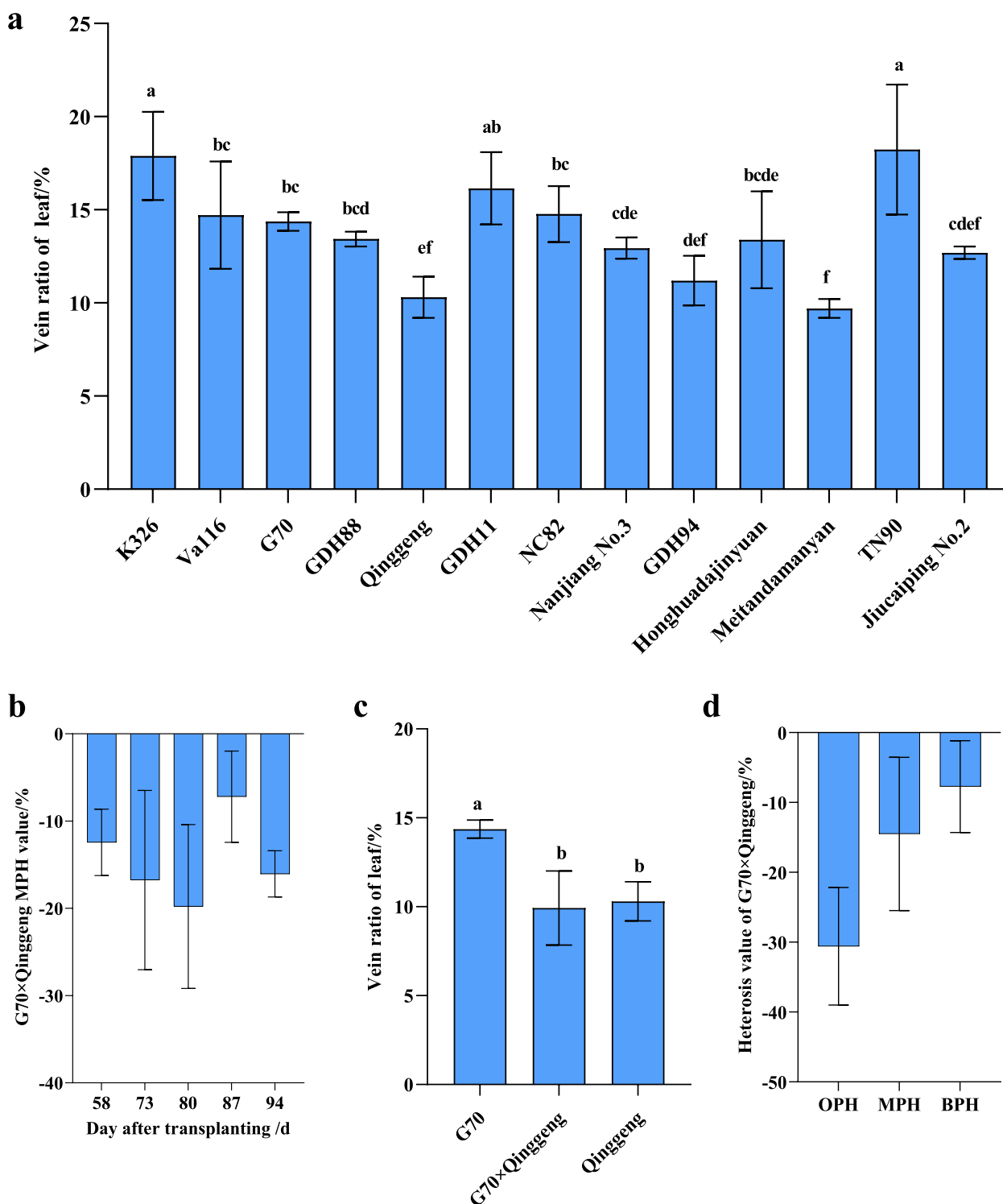


Fig. 1 The characteristics of leaf vein ratio and leaf vein ratio heterosis in different tobacco materials. The significant difference in leaf vein ratio was determined using Duncan's new multi range test method. Different lowercase letters represents significant difference ($P < 0.05$). The data plotted in the figure is the mean \pm standard error. **a** The results of leaf vein ratio in 13 parent materials. **b** Heterosis performance value of vein ratio of leaves in hybrid F_1 of the G70 x Qinggeng at 58th, 73th, 80th, 87th, and 94th day after transplanting. **c** Leaf vein ratio in tobacco hybrid G70 x Qinggeng and its parents. **d** Heterosis performance value of vein ratio of leaves in hybrid F_1 of G70 x Qinggeng. The OPH, MPH, and BPH represent over high parental heterosis, medium parental heterosis and low parental heterosis respectively. Figures were generated using GraphPad Prism 9

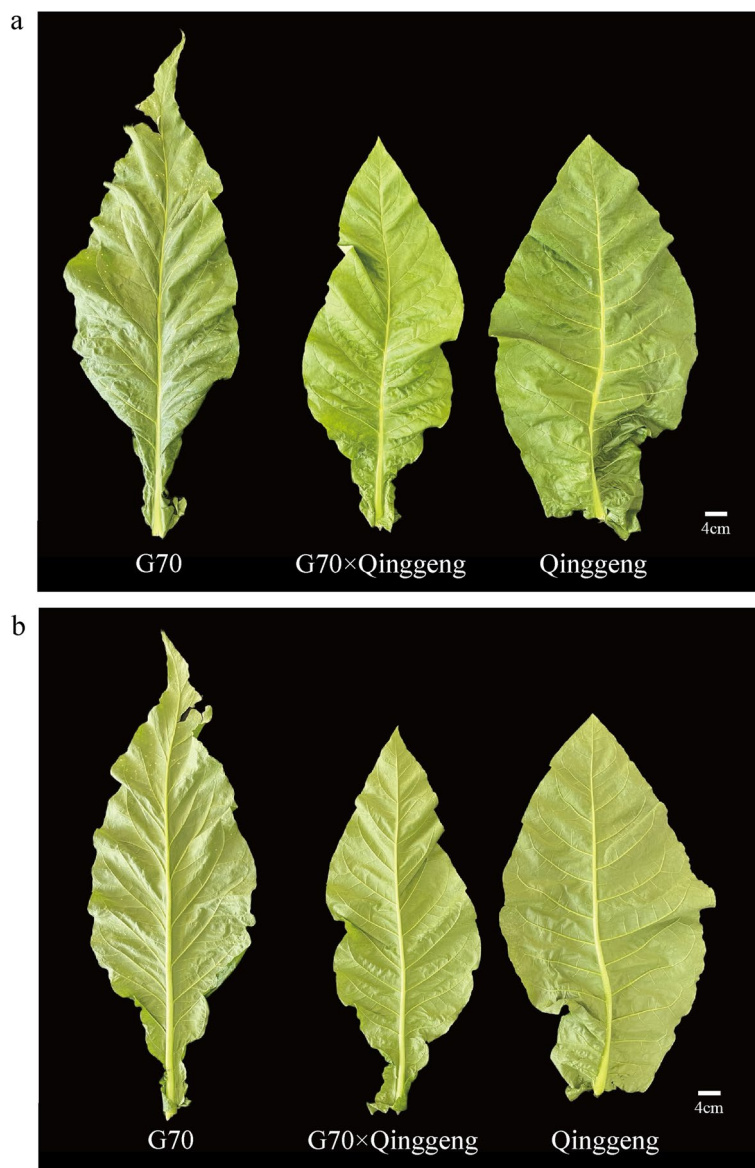


Fig. 2 The 10th leaf position fresh leaf images of hybrid G70×Qinggeng and its parents. **a** Front view of blade. **b** Blade back view

were dominant. The genes at P7–P12 showed transgressive expression, and the genes at P7–P9 showed down-regulated overdominance, whereas the genes at P10–P12 showed upregulated overdominance. The numbers of genes with different expression patterns are shown in Fig. 5b. Among the 12 expression patterns, P2 and P6 had the highest number of genes, with 326 and 203 genes, respectively. P8 and P5 contained the least number of genes (28 and 35, respectively). Additive expression (P1–P2) and non-additive expression (P3–P12) had 491 and 828 genes, respectively (Fig. 5c). The proportion of non-additive expression (62.77%) was much higher than that of additive expression (37.23%). Among the non-additive

expression patterns, the dominant expression pattern (P3–P6) exhibited a high proportion (39.04%). This result revealed that non-additives play a vital role in leaf vein ratio heterosis, especially in the dominant expression patterns.

Functional enrichment analysis of non-additive expressed genes

Numerous studies have underscored the vital role played by non-additively expressed genes in hybrid offspring performance. We conducted Gene Ontology (GO) and Kyoto Encyclopedia of Genes and Genomes (KEGG) enrichment analyses on 828 non-additive genes

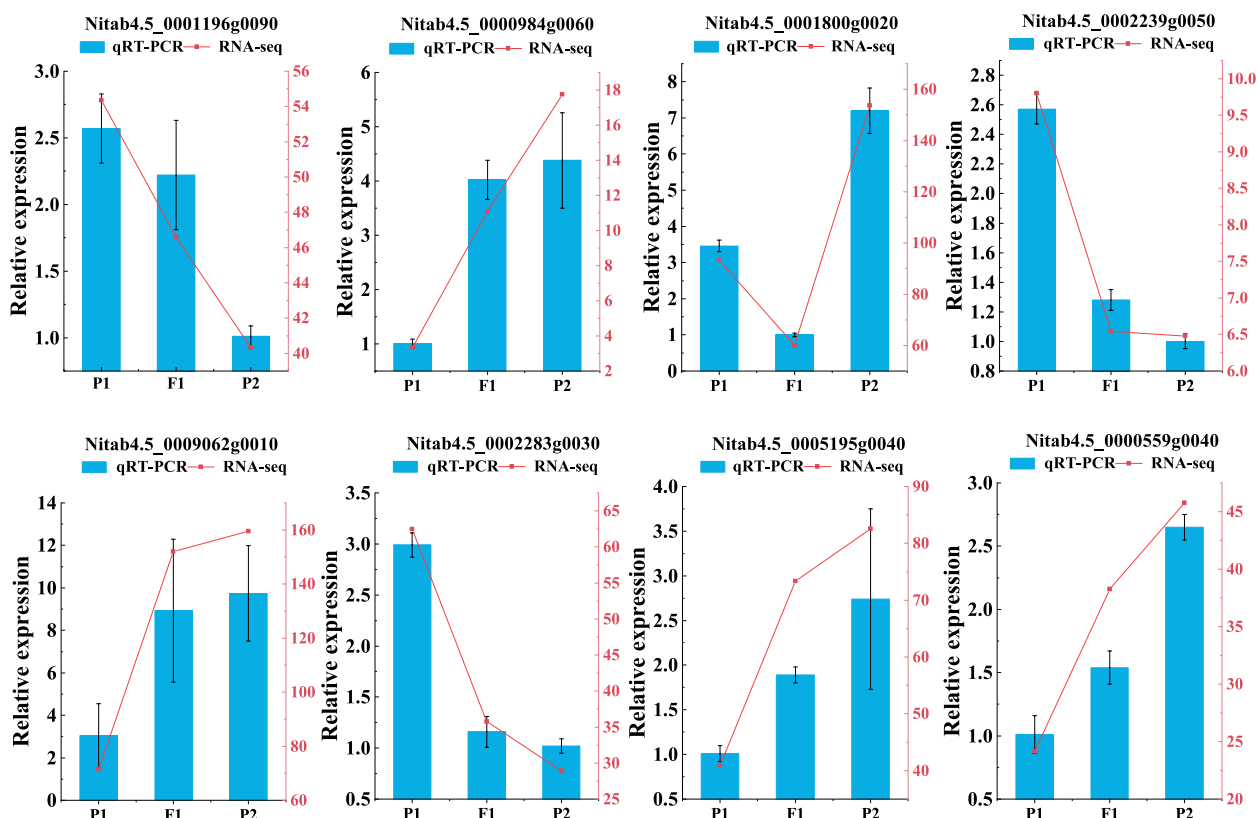


Fig. 3 Comparison of RNA-seq and qRT-PCR gene expression between G70 x Qinggeng and its parents. G70 = P1, Qinggeng = P2, and F₁ = G70 x Qinggeng

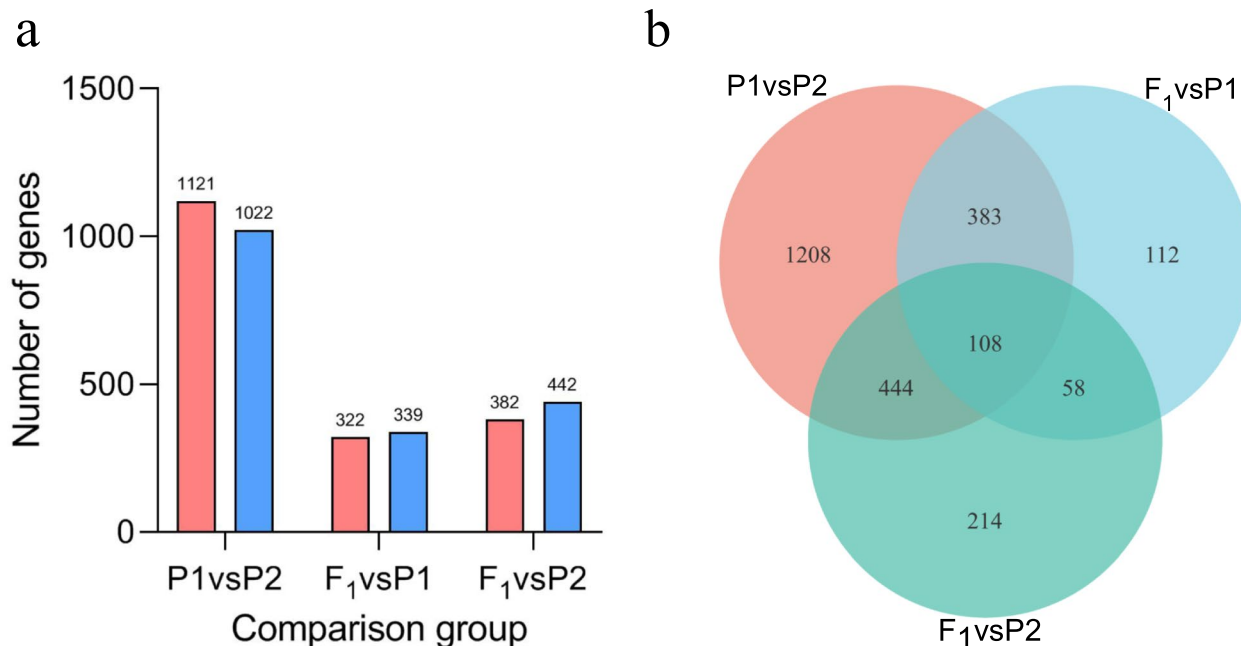


Fig. 4 The identification of DEGs and Venn diagrams of upregulated or downregulated gene expression in G70 x Qinggeng hybrids and parents. **a** The identification the upregulated and downregulated DEGs in the F₁ hybrids and parents. Red and blue columns represent upregulated and downregulated DEGs, respectively. **b** Venn diagram of differential expression in the F₁ hybrids and their parents. G70 = P1, Qinggeng = P2 and F₁ = G70 x Qinggeng

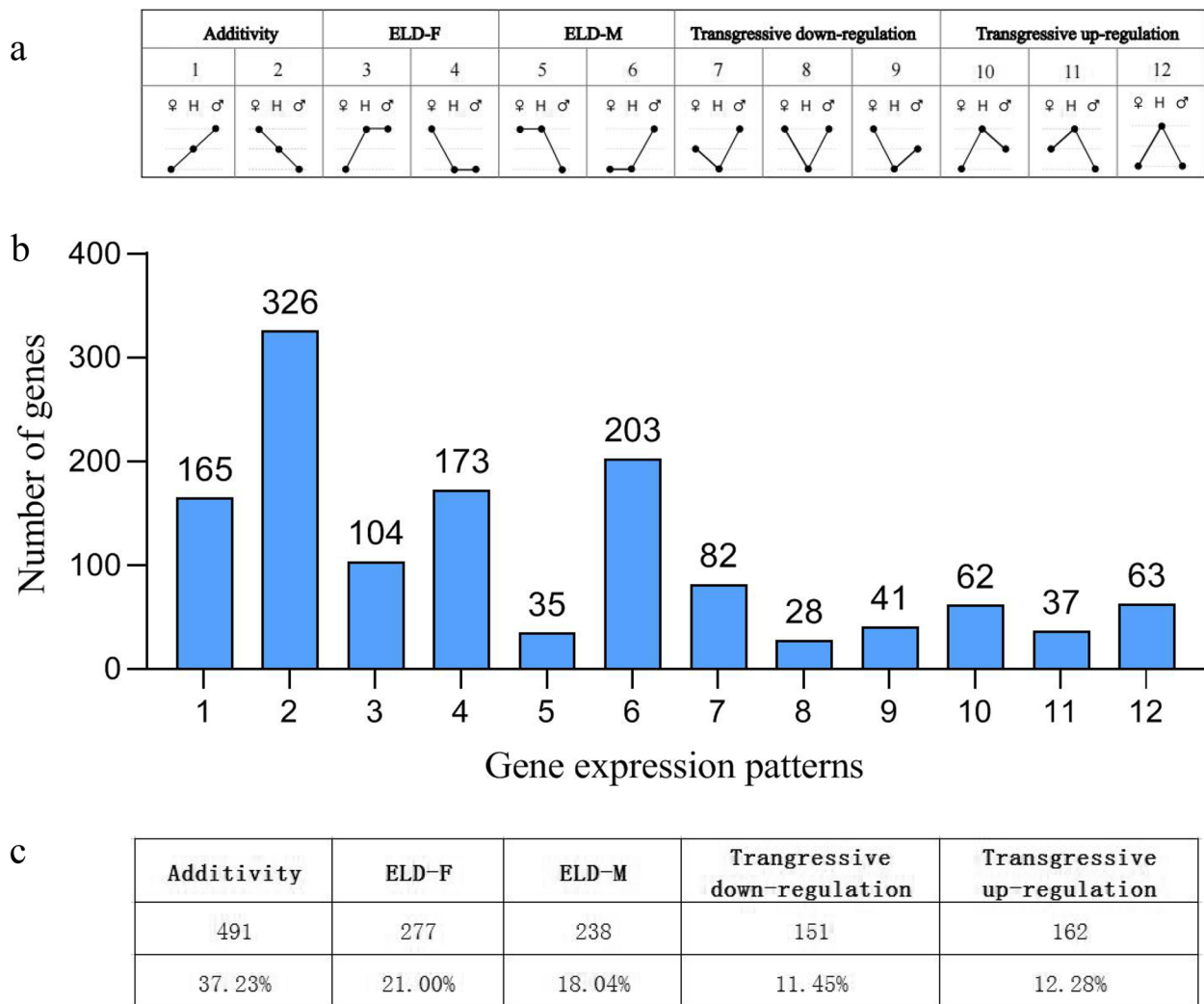


Fig. 5 Classification of 12 DEG expression patterns of differentially expressed genes in F₁ hybrids compared to their parents. **a** Expression patterns of 12 differentially expressed genes. ♂: male parent; H: hybrid; ♀: female parent. **b** The number of genes in each of the 12 hybrid expression patterns. **c** Numbers and proportions of the five total expression patterns in differentially expressed genes

to comprehend their physiological functions better. The GO enrichment results (Fig. 6a, Additional file 8) indicated that among the 828 genes, 709 were enriched across biological processes, cellular components, and molecular functions. Notably, the molecular functions category exhibited the most significant enrichment among these genes. The 709 genes were particularly enriched in functions associated with responses to abiotic stimuli, galactose metabolic processes, plant-type cell wall organization, auxin-activated signaling pathways, hydrolase activity, UDP-glycosyltransferase activity, and other GO terms (Fig. 6a). These results emphasized the significant role of these non-additive genes in influencing the leaf vein ratio.

Moreover, the KEGG enrichment analyses (Fig. 6b, Additional file 9) revealed that among the 828 genes, 359 were associated with 96 KEGG pathways. The first-level classification showed that a majority of the differentially expressed genes (DEGs) were involved in metabolism (196, 54.59%), genetic information processing (113, 31.48%), environmental information processing (22, 6.13%), cellular processes (16, 4.46%), and organismal systems (12, 3.34%). Specifically, the non-additive DEGs were prominently enriched in pathways such as phenylpropanoid biosynthesis, galactose metabolism, plant hormone signal transduction, glutathione metabolism, MAPK signaling pathway, plant starch, and sucrose metabolism (Fig. 6b). The top 20 KEGG pathways with

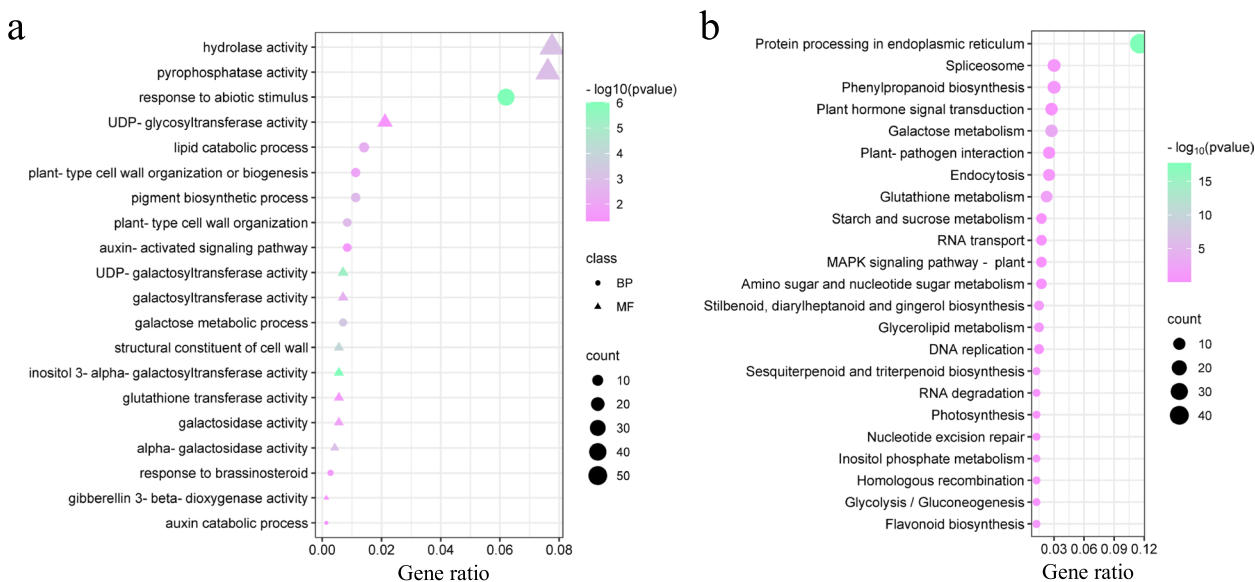


Fig. 6 Enrichment analysis of dominantly expressed genes. **a** GO enrichment analysis of non-additively expressed genes in hybrids and parents. **b** KEGG enrichment pathway analysis of non-additively expressed genes in hybrids and parents. Figures were drawn using a bioinformatics website (<https://www.bioinformatics.com.cn/>)

the highest enrichment level were shown in Additional file 10. These findings suggest that the expression of these non-additive DEGs regulates vital biological processes in hybrids, contributing to leaf development and regulation of the leaf vein ratio in hybrids.

Mining of key regulatory genes for vein ratio of leaves in hybrid

In order to further analyze the formation basis of vein-specific heterosis, we conducted annotation analysis and homologous comparison of important genes in the KEGG pathway associated with leaves (Table 1; Additional File 11). Plant hormones are commonly present in plants and participate in multiple growth and development processes. We found three *AUX/IAA* genes (LOC104109697; LOC104231359; LOC104111767) were over dominant downregulation expression. There were two ethylene-responsive transcription factors (LOC104109693; LOC104115628; LOC104109693) were dominant downregulation expression and one (LOC125862211) was overdominant downregulation expression. And one gibberellin (*GA*) gene (LOC104112986) were overdominant downregulation expression in this study. 24 xylose-transglucosylase/hydrolase proteins involved in the construction and remodeling of cellulose/xyglucan crosslinks, which play important roles in regulating cell-wall ductility, were downregulated in the hybrid. Many transcription factors related to the leaf development showed dominant or over-dominant downregulation in hybrid, such as MYB(LOC109235261), bHLH(LOC104245010; LOC107813550), bZIP(LOC107813846; LOC107781357; LOC107804246; LOC104228318; LOC104221704). Cytochrome

P450, which is involved in leaf development and senescence. There were four cytochrome P450 genes (LOC104084433; LOC104112316; LOC104241840; LOC104241840) were overdominant downregulated in the hybrid. We selected six genes related to leaf vein ratio and transport for qRT-PCR analysis (Fig. 7). These genes and their corresponding primers are listed in Additional File 12. The results showed that the expression levels of these genes in the G70×Qinggeng hybrid were significantly lower than those in the two parental inbred lines, indicating that these genes had significant overdominant and dominant expression patterns in the hybrid. These results suggest that overdominant and dominant downregulation of key genes related to leaf vein ratio leads to leaf vein ratio heterosis.

Discussion

Heterosis refers to the enhanced performance of offspring in desired traits compared to either parent [3]. The utilization of hybrid vigor breeding has successfully leveraged heterosis advantages to improve worldwide crop quantity and quality [15, 49, 50]. Numerous studies have investigated hybrid vigor various such as rice [15], wheat [51], cotton [52], *A. thaliana* [53], maize [54], and *Brassica napus* [55]. The advancement of quantitative genetics, molecular genetics, and genomics has led to the utilization of experimental techniques including transcriptomics [53, 56], metabolomics [57], and proteomics [23, 58] to elucidate the mechanisms of heterosis formation. The incorporation of transcriptome analyses into heterosis research has offered valuable molecular insights

Table 1 Statistics of genes related to vein ratio of leaves heterosis

Pattern	Gene symbol	Description	F ₁	P1	P2	MP	FC	H_FPKM
Dominant	LOC104109693	ethylene-responsive transcription factor TINY isoform X1	0.02	1.99	0.03	1.01	0.02	-97.68
	LOC104115628	ethylene-responsive transcription factor ERF056-like	1.78	21.28	1.25	11.27	0.16	-84.17
	LOC104245010	transcription factor bHLH110-like	0.53	1.86	0.64	1.25	0.43	-57.39
	LOC104228318	receptor-like serine/threonine-protein kinase ERECTA isoform X2	5.76	17.44	6.08	11.76	0.49	-51.03
	LOC107783985	allene oxide synthase, chloroplastic-like	1.59	7.39	1.98	4.68	0.34	-66.12
	LOC107804012	beta-amyrin 28-oxidase-like	0.95	1.27	3.11	2.19	0.43	-56.71
	LOC104107783	xyloglucan endotransglucosylase/hydrolase protein 24-like	11.53	50.99	9.59	30.29	0.38	-61.95
Overdominant	LOC125862211	ethylene-responsive transcription factor TINY isoform X1	1.00	5.60	2.05	3.83	0.26	-73.95
	LOC104109697	auxin-responsive protein IAA27-like	3.31	9.78	5.30	7.54	0.44	-56.10
	LOC104231359	auxin-induced protein AUX22-like	104.73	162.87	299.05	230.96	0.45	-54.66
	LOC104111767	auxin-induced protein AUX22-like	8.38	12.12	23.57	17.85	0.47	-53.06
	LOC107813550	transcription factor bHLH137 isoform X2	1.09	1.81	2.07	1.94	0.56	-43.77
	LOC107813846	LRR receptor-like serine/threonine-protein kinase At3g47570	0.03	0.24	0.01	0.13	0.27	-73.33
	LOC107781357	LRR receptor-like serine/threonine-protein kinase EFR isoform X1	0.61	0.26	2.85	1.55	0.39	-60.73
	LOC107804246	bZIP transcription factor TGA10	0.03	0.49	0.09	0.29	0.10	-89.71
	LOC104221704	leucine-rich repeat receptor-like protein kinase At1g35710	0.50	1.49	0.35	0.92	0.54	-45.85
	LOC109235261	myb family transcription factor EFM-like	0.57	5.60	1.96	3.78	0.15	-85.02
	LOC104084433	cytochrome P450 CYP82D47-like	0.11	0.58	0.41	0.50	0.22	-78.45
	LOC104112316	cytochrome P450 CYP72A219-like	0.88	1.59	7.96	4.78	0.18	-81.51
	LOC104240584	cytochrome P450 716B1-like	0.98	0.74	2.36	1.55	0.63	-36.91
	LOC104241840	cytochrome P450 superfamily	0.03	6.56	0.03	3.30	0.01	-99.09
	LOC107778026	alkane hydroxylase MAH1-like	0.77	1.46	2.67	2.07	0.37	-62.90
	LOC104112986	snakin-2	219.15	784.81	629.42	707.12	0.31	-69.01

MP represents the average value of gene expression of two parents G70 and Qinggeng

FC represents the foldchange of hybrid combination G70×Qinggeng, and H_FPKM represents the heterosis value of gene expression

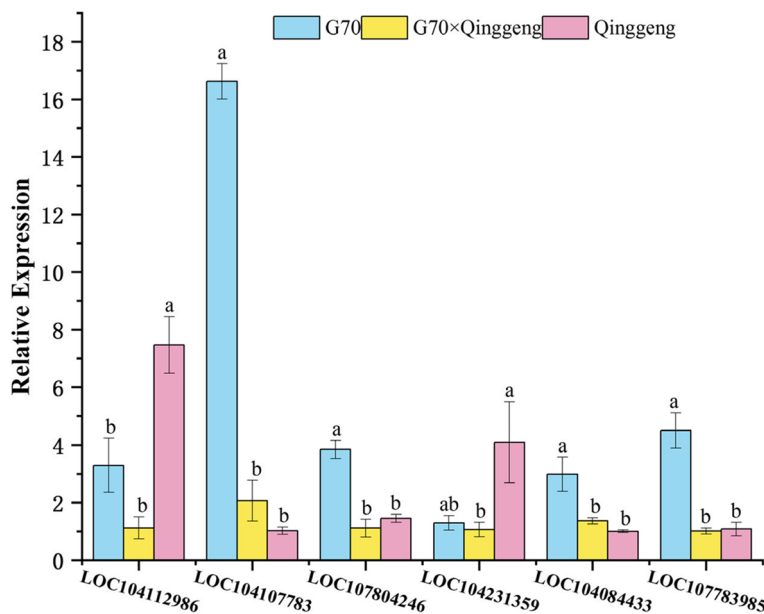


Fig. 7 Expression level analysis of vein ratio of partial leaf genes using qRT-PCR. Different lowercase letters represent significant ($P < 0.05$). The data plotted in the figure is the mean \pm standard error

into various plant species, including *A. thaliana*, rice [6, 22], maize [25, 49], Chinese cabbages [14], easter lily [27] and tobacco [23, 59]. However, the molecular basis of leaf vein ratio in tobacco remains unexplored. The high vein ratio found in tobacco leaves, attributed to the dense and thick tissue structure of veins, creates challenges during cigarette processing. Disposal of these leaves contributes to environmental pollution and adversely affects the quality, cost, and profitability of cigarette production. Hence, our research aims to investigate the genetic mechanisms of heterosis in achieving low leaf vein ratios in F₁ hybrids and their parent plants using a comparative transcriptome analysis.

Our study identified 661 and 824 DEGs in the F₁ hybrid (G70×Qinggeng) and its respective inbred parents. We observed a higher count of downregulated DEGs compared to than upregulated ones. This suggests that downregulated genes might contribute to the strong negative heterosis observed in the tobacco leaf vein ratio. Analysis of the 1319 common DEGs between hybrids and parents revealed that a higher number of non-additively expressed genes (828) compared to additively expressed ones (491). The analysis of 828 DEGs revealed that 277 were dominantly expressed in the hybrid line, whereas 238 showed dominant expression in the parental lines. Among the 1319 DEGs, 39.04% were identified as dominant genes, highlighting their collaborative role in tobacco leaf vein ratio heterosis. Previous research on crop heterosis has consistently highlighted the significance of dominant gene expression. For example, a study on Chinese cabbage hybrids revealed that more than 81% of differentially expressed genes exhibited dominance [13]. An analysis of upland cotton hybrids using transcriptome technology indicated that a significant proportion of hybrids displayed a preference for DEGs in comparison to their parental varieties [26]. Yu et al. [60] demonstrated in their research on rice heterosis that four QTLs exhibited a mode of dominance or superdominance. Shen et al. [61] noted in their research on *B. napus* hybrid and found that high parental expression-level dominance played an important role in heterosis. Overall, the expression of dominant genes significantly impacts leaf vein ratio heterosis..

Plant hormone signal transduction pathways, including tryptophan metabolism (auxin), zeatin biosynthesis (cytokine), dilt biosynthesis (gibberellin), carotenoid biosynthesis (abscisic acid), brassinosteroid biosynthesis (brassinosteroid), α -linolenic acid metabolism (jasmonic acid), and phenylalanine metabolism (salicylic acid), play an important role in repulating various plant growth and development processes. These processes include plant cell division, embryogenesis, morphogenesis, sexual response, prolonged dormancy, apical dominance, and

tissue differentiation. The plant hormone auxin, known as indole-3-acetic acid (IAA), plays a crucial role in regulating various stages of plant growth and development, from embryogenesis to senescence. It modulates the expression of downstream genes that code for proteins involved in a diverse array of physiological processes [62, 63]. Auxins play a crucial role in plant growth and development by directly or indirectly influencing the development of plant leaf veins [64]. Research on the *dl2* rice mutant has demonstrated that the polar transport and distribution of auxin play a crucial role in regulating the mid-vein ratio and nutritional growth of rice leaves [65]. Previous studies have demonstrated that the absence of IAA9 can induce the conversion of compound tomato leaves into single leaves, while the upregulation of IAA9 expression can enhance leaf vascularization [66]. This indicated that IAA9 is a key mediator of leaf morphogenesis. Our study observed reduced expression levels of IAA (LOC104109697, LOC104231359, and LOC104111767) in hybrids compared to the parental inbred lines, exhibiting downregulated over-dominant expression. The lower expression of IAA genes in hybrid might contribute to manifestation of heterosis in leaf vein ratio.

The APETALA2/ethylene-responsive factor (AP2/ERF) superfamily, predominantly identified in plants, is recognized as one of the largest transcription factor families. It is widely involved in important biological processes, such as plant growth and development, the regulation of secondary metabolism, and responses to both biotic and abiotic stress [67, 68]. AP2/ERF transcription factors are categorized into five primary groups based on the number and similarity of AP2 domains they harbor: AP2 (APETALA2), dehydrogenation-responsive element-binding proteins (DREB), ethylene-responsive factor (ERF), Related to AB13/VP (RAV), and the Soloist subfamily [69]. Jiang et al. [70] found that mutations in an AP2 transcription factor-like gene affected maize internode length and leaf shape. Moreover, the study on *A. thaliana* revealed that the upregulation of *DEAR4* correlated with leaf senescence and could be triggered by ABA, JA, darkness, drought, and salt stress. After leaf aging, degradation of certain mesophyll substances results in an increased leaf-vein ratio. Our research revealed a decrease in the dominant or overdominant expression of ethylene-related genes in the hybrid. We hypothesize that this downregulation could explain the negative heterosis observed in the vein ratio of tobacco leaves.

Gibberellic acid (GA) is a phytohormone crucial for various aspects of plant development [71]. Fundamental roles of GAs have been identified in almost every phase of plant development, including seed germination [72], flowering [73], leaf expansion [74], leaf formation [75],

leaf angle [76], leaf size [77], and senescence [78]. Various factors such as bioactive GAs, GA biosynthesis genes, DELLAs, light, TFs, phytohormone crosstalk, and other proteins are involved in regulating leaf size by affecting cell size, cell number, and the size of the leaf [79]. Therefore, the gene (LOC104112986) related to GAs exhibited overdominant downregulation in the hybrid, leading to the generation of a major vein ratio in tobacco leaves.

Xyloglucan is the main hemicellulose present in the primary cell walls of dicotyledonous and non-gramineous monocotyledonous plants [80]. Xyloglucan endotransglucosylase/hydrolase (XTH) is a cell-wall-relaxation factor found in diverse plant tissues and cells. Its function includes modifying the structure of cellulose–xylan complex by catalyzing the breaking and rejoining of xyloglucan molecules within the plant cell wall [81]. XTH is a crucial enzyme involved in the remodeling of plant cell wall. The XTH family consists of multiple members, and exhibiting diverse expression profiles in different plant tissues and developmental stages. These enzymes play essential roles in plant growth and development, impacting functions in roots, stems, leaves, flowers, and fruit ripening. The *XTH* gene in *A. thaliana*, exhibits significant expression of *AtXTH27* in leaf vein guiding tissues and extended rosette leaves, with the deletion mutation of *AtXTH27* leading to shortened of the tertiary leaf vein ducts [82]. In tobacco, the *NtXTH* gene (LOC104107783) regulates vein ratio by influencing leaf vein development. Suppression of *NtXTH* gene expression in hybrids is linked to a decrease in major vein ratios of leaves, along with an enhancement in plant-type cell wall organization as revealed by GO enrichment analysis.

Transcription factors (TFs) play important roles in several biochemical and physiological processes in numerous tissues at different developmental stages, such as seed germination, flowering time regulation, shade avoidance, and stress responses [83, 84]. The basic helix-loop-helix (bHLH) family, the second largest TF group in plants, significantly influences plant growth, development, and stress responses [85]. In *A. thaliana*, the overexpression of *Cibhlh027* resulted in accelerated leaf senescence, reduced chlorophyll content, enhanced ion permeability, and increased cell death [86].

The *HD-ZIP III* gene plays a crucial role in the regulation of leaf vein development in plants. There are five *HD-ZIP III* genes in *A. thaliana*, namely *PHB*, *REV*, *CNA*, *ATHB15*, and *ATHB8*. *ATHB8* exhibits specific expression in precursor and procambium cells, directly regulated by MONOPTEROS (MP) [87]. The expression of *ATHB8* is regulated by MP through its binding to the auxin-responsive element TGTCTG (ARE). The investigation of the *mp/athb8* dual mutant indicated

that *ATHB8* acts on the downstream regulation of leaf vein development in MP [87]. Our study found that the expression levels of five genes associated with the regulation of leaf vein development in F₁ hybrids were lower than those in the two parents, indicating a negative expression advantage.

The MYB transcription factor family, one of the largest transcription factor families in plants [88, 89], plays key roles in plant development, metabolism, and stress tolerance, with *AtMYB91/ASI* being specifically involved in leaf patterning regulation [90, 91]. *AtMYB2* regulates leaf senescence, while *AtMYB44/MYBRI* plays a role in the regulatory pathways of leaf senescence and ABA signaling [92, 93]. By examining the expression patterns in diverse tissues, it was revealed that *BcMYB101* has higher transcript levels in petioles, leaves, roots, and floral organs. The overexpression of *BcMYB101* was found to enhance leaf number and result in the downward curling of cauline leaves [94]. Additionally, the findings indicated that LOC109235261, which is involved in leaf development and senescence, showed decreased dominant expression in the hybrid.

The *CYP78A* family (*CYP78As*) is a plant-specific gene family highly conserved among terrestrial plants [95]. *AtKLU/AtCYP78A5* regulates the growth of leaves, flowers, grains, siliques, and other organs by modulating cell division [96–99]. The *klu* loss-of-function mutants produce smaller leaves and floral organs because of the inhibition of cell division [97]. Mutant analyses revealed that *AtKLU*, *AtCYP78A7*, and *AMP1* (*Altered meristem program1*) regulate plastochron length and leaf senescence in the same genetic pathway in *A. thaliana*. Christ et al. [100] revealed that the cytochrome P450 CYP89A9 is involved in the formation of major chlorophyll catabolites during leaf senescence in *A. thaliana*. In this study, the overdominant downregulation expression of four genes related to cytochrome P450 in the hybrid F₁ results in a negative heterosis of the vein ratio of tobacco leaves.

The study offers insights into the intricate regulatory process of heterosis in crops, shedding light on the mechanism underlying leaf vein ratio heterosis in tobacco at the transcriptional level. This research opens a new avenue for understanding and potentially cultivating tobacco varieties with reduced leaf vein ratios. The leaf vein ratio, intricately linked with leaf morphology, size, and senescence, is notably influenced by gene expression related to these physiological functions. The hybrid's low expression of genes associated with these functions contributes to the manifestation of negative heterosis in the leaf vein ratio, thereby prominently displaying negative heterosis in this trait.

Materials and methods

Plant materials, growth conditions, and analysis of leaf vein ratio of leaves

In this study, 13 tobacco materials with distinct leaf vein ratios served as parental lines, while 12 hybrid combinations were generated to investigate leaf vein ratio heterosis. These materials, acquired from the Guizhou Key Laboratory of Tobacco Quality Research, were cultivated at the Guizhou University Tobacco Research Base starting in 2021. The seeds were initially planted in a specialized substrate for flue-cured tobacco and nurtured in a growth room until they reached the stage of having five true leaves before being transplanted to the field. The field trial was conducted using a randomized block design with three biological replicates, each comprising 45 individual plants. The spacing between rows and inter-row spacing was set at 110 cm and 55 cm, respectively. Topping of all materials occurred on the same day once over 50% of the plants had bloomed (73 days after transplanting). At 58, 73, 80, 87, and 94 d post-transplanting from the main veins and mesophyll between the 6th and 8th branches of the 9th to 11th leaf positions. For each collection, three randomly selected thriving plants from each batch were used for mixed sampling. Fresh samples were rapidly frozen in liquid nitrogen and subsequently preserved in an ultra-low-temperature refrigerator at -80°C for qRT-PCR and transcriptomic analysis. The remaining leaf samples were subjected to denaturation at 105°C for 30 min followed by drying at 75°C . The leaf vein ratio was calculated based on the method described by Que et al. [101].

RNA isolation and sequencing

Total RNA was extracted from the leaf tissue using TRIzol[®] Reagent (Plant RNA Purification Reagent for plant tissue) according to the manufacturer's instructions (Invitrogen). RNA quality was determined using a 2100 Bioanalyzer (Agilent) and quantified using an ND-2000 (NanoDrop Technologies). All of the RNA samples were collected in high-quality situations ($\text{OD}_{260}/\text{OD}_{280} = 1.8 \sim 2.2$, $\text{OD}_{260}/\text{OD}_{230} \geq 2.0$, $\text{RIN} \geq 6.5$, $28\text{S}:18\text{S} \geq 1.0$, $> 1 \mu\text{g}$). RNA-seq transcriptome library was prepared following TruSeq[™] RNA sample preparation Kit from Illumina (San Diego, CA) using $1 \mu\text{g}$ of total RNA. First, mRNA was isolated according to the poly-A selection method using oligo(dT) beads and then fragmented using fragmentation buffer. Next, double-stranded cDNA was synthesized using a SuperScript double-stranded cDNA synthesis kit (Invitrogen, Carlsbad, CA, USA) with random hexamer primers (Illumina). Then the synthesized cDNA was subjected to end-repair, phosphorylation, and 'A' base addition according to Illumina's library construction protocol. Libraries were selected for

cDNA target fragments of 300 bp on 2% low-range ultra-agarose, followed by PCR amplification using Phusion DNA polymerase (NEB) for 15 PCR cycles. After quantification using TBS380, the paired-end RNA-seq library was sequenced using an Illumina HiSeq xten/NovaSeq 6000 sequencer (2×150 bp read length).

Transcriptomics data processing and analysis

Raw paired-end reads were trimmed and quality was controlled using SeqPrep. (<https://github.com/jstjohn/SeqPrep>), and Sickle (<https://github.com/najoshi/sickle>) with default parameters. Clean reads were separately aligned to the K326 genome (https://solgenomics.net/organism/Nicotiana_tabacum/genome) in orientation mode using the HISAT2 (<http://ccb.jhu.edu/software/hisat2/index.shtml>) software [102]. The mapped reads of each sample were assembled using StringTie (<https://ccb.jhu.edu/software/stringtie/index.shtml>). $t = \text{example}$, using a reference-based approach [103]. To identify DEGs (differentially expressed genes (DEGs)) between the two samples, the expression level of each transcript was calculated according to the transcripts per million reads (TPM) method. RSEM (<http://deweylab.biostat.wisc.edu/rsem/>) [104] was used to quantify gene abundance. Essentially, differential expression analysis was performed using the DESeq2 [105] with $\text{padjust} \leq 0.05$, DEGs with $|\log_2\text{FC}| \geq 1$ were considered to be significantly different expressed genes. In addition, functional-enrichment analysis including GO and KEGG was performed to identify which DEGs were significantly enriched in GO terms and metabolic pathways at Bonferroni-corrected $P\text{-value} \leq 0.05$ compared with the whole-transcriptome background. GO functional enrichment and KEGG pathway analyses were performed using Goatools (<https://github.com/tanghaibao/Goatools>) and KOBAS (<http://kobas.cbi.pku.edu.cn/home.do>) [106]. Transcription factor analysis was performed by using the plant transcription factor database (PlantTFDB) with Hmmscan E-value and Blast E-value parameters were both set to less than or equal to $1.0\text{E-}5$.

qRT-PCR

To validate the expression levels of tobacco genes derived from RNA sequencing, we performed Real-time PCR (qRT-PCR) experiments using the BIO-RAD CFX96 Real-Time qRT-PCR system. Randomly selected genes were analyzed, and the specific primers used for qRT-PCR are listed in Additional Files 5 and 12. The qRT-PCR analysis, conducted using Talent qRT-PCR PreMix (SYBR Green) from TIANGEN (FP209) underwent 3 biological repetitions with 3 technical replicates. Final test results were calculated using the $2^{-\Delta\Delta\text{Ct}}$ method [107].

Results from real-time PCR for all genes are presented as average values along with their standard errors.

Statistical analysis

The field experiment design was randomized with three replicates. DPS (Data Processing System) software was used to analyze the variance of the data (ANOVA). The variance analysis was determined using Duncan's new multiple range test method. Different lowercase and uppercase letters indicate significant ($P < 0.05$). Over high-parent heterosis (OPH), mid-parent heterosis (MPH), and below low-parent heterosis (BPH) was calculated as follows: $OPH(\%) = (F_1 - HP) / HP \times 100$, $MPH(\%) = (F_1 - MP) / MP \times 100\%$, $BPH(\%) = (F_1 - LP) / LP \times 100\%$, where; F_1 = performance of the hybrid, HP = high-value parent, mid-parent average (MP) = $(P_1 + P_2) / 2$, LP = low-value parent. In the analysis of gene expression advantage, MP is the average expression level of a certain gene in both parents $((P_1 + P_2) / 2)$, and FC is the ratio of the expression level of a certain gene in F_1 to the expression level in both parents ($FC = F_1 / MP$). H FPKM refers to the heterosis value of gene expression, calculated using the formula for heterosis calculation $((F_1 - MP) / MP \times 100\%)$.

Conclusion

Leaves function as the primary organs for photosynthesis in higher plants. The occurrence and development of leaf veins are closely associated with leaf growth, serving a crucial role in transporting water and nutrients while providing structural support during development. Given the need to minimize economic costs and resource wastage in the tobacco industry, there's a growing demand for tobacco varieties with reduced leaf vein ratios. This study conducted a comparative transcriptome analysis of leaf vein ratio heterosis observed in the hybrid and its parental lines. Broadly, non-additive genes emerged as significant contributors to leaf vein ratio heterosis, particularly dominantly expressed genes, which constituted the majority. Among these dominant genes, several were found to encode plant hormones. These identified differentially expressed genes (DEGs) might actively contribute to the observed leaf vein ratio heterosis in tobacco plants. Consequently, this extensive research presents novel insights into the molecular mechanisms underpinning leaf vein ratio heterosis in tobacco. These findings hold promise as a valuable resource for further molecular investigations aimed at breeding tobacco varieties with reduced leaf vein ratios.

Abbreviations

DEGs	Differentially expressed genes
qRT-PCR	Real-time fluorescence quantitative PCR
MPH	Mid-parent heterosis
OPH	Over-high parent heterosis

BPH	Below low parental heterosis
GO	Gene Ontology
KEGG	Kyoto Encyclopedia of Genes and Genomes
bZIP	Basic leucine zipper
MYB	V-myb avian myeloblastosis viral oncogene homolog
bHLH	Basic helix-loop-helix
QTL	Quantitative trait locus
TF	Transcription factor
GA	Gibberellin
AP2/ERF	APETALA2/ethylene-responsive factor
XTH	Xyloglucan endotransglucosylase/hydrolase

Supplementary Information

The online version contains supplementary material available at <https://doi.org/10.1186/s12864-024-10821-1>.

Additional File 1: Table S1. Heterosis value of the vein ratio of leaves in tobacco of 12 hybrids.

Additional File 2: Table S2. Heterosis values of leaf vein ratio with G70 × Qinggeng in 2020 and 2021.

Additional File 3: Table S3. Transcriptome quality control data.

Additional File 4: Table S4. Overview of the RNA sequencing data for all nine transcriptomes.

Additional File 5: Table S5. Primer sequences for qRT-PCR.

Additional File 6: Table S6. 8 genes expression levels by qRT-PCR.

Additional File 7: Table S7. Information table of 1319 differential genes between F_1 and parents.

Additional File 8: Table S8. GO enrichment information for 828 non-additive-expressed DEGs.

Additional File 9: Table S9. KEGG enrichment information for 828 non-additive-expressed DEGs.

Additional File 10: Figure S1. The top 20 KEGG pathways with the highest enrichment level.

Additional File 11: Figure S2. Protein sequences alignment map of key genes.

Additional File 12: Table S10. Primer sequences of partial genes related to the vein ratio of leaf heterosis for qRT-PCR.

Acknowledgements

We thank all of our colleagues who participated in this study and provided constructive suggestions.

Authors' contributions

LLD planned and designed the research, analyzed the data, and wrote the manuscript. ZJM, KYL, KP, and JYL performed most of the fieldwork. YHQ, QZ, JYZ, and GZW carried out the molecular biology and chemistry studies. RXL supervised the study and participated in its design and coordination. All the authors reviewed and approved the final manuscript.

Funding

This study was financially supported by the National Science Foundation of China (32060510) and Science and Technology Project of the Guizhou Tobacco Company (2022XM02). These funding bodies were not involved in the study design, collection, analysis, interpretation of data, writing of this article, or the decision to submit it for publication.

Availability of data and materials

Whole *Nicotiana tabacum* genome sequence information was obtained from the solgenomics website (https://solgenomics.net/organism/Nicotiana_tabacum/genome), which is available to all researchers. All the tobaccomaterials used in this study were supplied by Prof. Liu Renxiang of Guizhou University. The datasets supporting the conclusions of this study are included in the article and the Additional Files. The sequencing database of the parents

and hybrids has been deposited at NCBI under the GEO accession number (GSE246929) <https://www.ncbi.nlm.nih.gov/geo/query/acc.cgi?acc=GSE246929>.

Data availability

The sequencing database of the parents and hybrids has been deposited at NCBI under the GEO accession number (GSE246929) <https://www.ncbi.nlm.nih.gov/geo/query/acc.cgi?acc=GSE246929>.

Declarations

Ethics approval and consent to participate

Not applicable.

Consent for publication

Not applicable.

Competing interests

The authors declare no competing interests.

Received: 22 December 2023 Accepted: 20 September 2024

Published online: 03 October 2024

References

- Tester M. Breeding Technologies to Increase. *Science*. 2010;818:818–22. <https://www.sciencemag.org/cgi/content/abstract/327/5967/818>.
- Jin J, Sun Y, Qu J, Syah R, Lim CH, Alfiko Y, et al. Transcriptome and functional analysis reveals hybrid vigor for oil biosynthesis in oil palm. *Sci Rep*. 2017;7:1–12. <https://doi.org/10.1038/s41598-017-00438-8>.
- Shalby N, Mohamed IAA, Xiong J, Hu K, Yang Y, Nishawy E, et al. Overdominance at the gene expression level plays a critical role in the hybrid root growth of brassica napus. *Int J Mol Sci*. 2021;22(17):9246. <https://doi.org/10.3390/ijms22179246>.
- Paschold A, Jia Y, Marcon C, Lund S, Larson NB, Yeh CT, et al. Complementation contributes to transcriptome complexity in maize (*Zea mays* L.) hybrids relative to their inbred parents. *Genome Res*. 2012;22:2445–54. <https://doi.org/10.1101/gr.138461.112>.
- Schnable PS, Springer NM. Progress toward understanding heterosis in crop plants. *Annu Rev Plant Biol*. 2013;64:71–88. <https://doi.org/10.1146/annurev-arplant-042110-103827>.
- Shao L, Xing F, Xu C, Zhang Q, Che J, Wang X, et al. Patterns of genome-wide allele-specific expression in hybrid rice and the implications on the genetic basis of heterosis. *Proc Natl Acad Sci U S A*. 2019;116:5653–8. <https://doi.org/10.1073/pnas.1820513116>.
- Bruce AB. The Mendelian theory of heredity and the augmentation of vigor. *Science*. 1910;32:627–8. <https://doi.org/10.1126/science.32.827.627-a>.
- Jones DF. Dominance of Linked Factors As a Means of Accounting for Heterosis. *Genetics*. 1917;2:609–609. <https://doi.org/10.1093/genetics/2.6.609a>.
- Minvielle F. Dominance is not necessary for heterosis: A two-locus model. *Genet Res*. 1987;49:245–7. <https://doi.org/10.1017/S0016672300027142>.
- Schnell FW, Cockerham CC. Multiplicative vs. arbitrary gene action in heterosis. *Genetics*. 1992;131:461–9. <https://doi.org/10.1093/genetics/131.2.461>.
- Younas A, Sadaqat HA, Kashif M, Ahmed N, Farooq M. Combining ability and heterosis for grain iron biofortification in bread wheat. *J Sci Food Agric*. 2020;100:1570–6. <https://doi.org/10.1002/jsfa.10165>.
- Zanewich KP, Rood SB. Gibberellins and heterosis in crops and trees: an integrative review and preliminary study with brassica. *Plants*. 2020;22(9):139. <https://doi.org/10.3390/plants9020139>.
- Li S, Jayasinghe CPA, Guo J, Zhang E, Wang X, Xu Z. Comparative transcriptomic analysis of gene expression inheritance patterns associated with cabbage head heterosis. *Plants*. 2021;10:1–20. <https://doi.org/10.3390/plants10020275>.
- Kong X, Chen L, Wei T, Zhou H, Bai C, Yan X, et al. Transcriptome analysis of biological pathways associated with heterosis in Chinese cabbage. *Genomics*. 2020;112:4732–41. <https://doi.org/10.1016/j.ygeno.2020.08.011>.
- Huang X, Feng Q, Qian Q, Zhao Q, Wang L, Wang A, et al. High-throughput genotyping by whole-genome resequencing. *Genome Res*. 2009;19:1068–76. <https://doi.org/10.1101/gr.089516.108>.
- Wang C, Tang S, Zhan Q, Hou Q, Zhao Y, Zhao Q, et al. Dissecting a heterotic gene through GradedPool-Seq mapping informs a rice-improvement strategy. *Nat Commun*. 2019;10(1):2982. <https://doi.org/10.1038/s41467-019-11017-y>.
- Huang X, Yang S, Gong J, Zhao Q, Feng Q, Zhan Q, et al. Genomic architecture of heterosis for yield traits in rice. *Nature*. 2016;537:629–33. <https://doi.org/10.1038/nature19760>.
- Mabire C, Duarte J, Darracq A, Pirani A, Rimbart H, Madur D, et al. High throughput genotyping of structural variations in a complex plant genome using an original Affymetrix® Axiom® array. *bioRxiv*. 2018;20:1–25. <https://doi.org/10.1101/507756>.
- ZhiLan X, KunLong H, LongJiang G, NanNan S, JiaBao W, BeiJiu C, et al. Transcriptome analysis of heterosis in maize (*Zea mays*) hybrid Longping206. *J Agric Biotechnol*. 2017;25:709–21. <https://doi.org/10.3969/j.issn.1674-7968.2017.05.003>.
- Baldauf JA, Vedder L, Schoof H, Hochholdinger F. Robust non-syntenic gene expression patterns in diverse maize hybrids during root development. *J Exp Bot*. 2020;71:865–76. <https://doi.org/10.1093/jxb/erz452>.
- Krieger U, Lippman ZB, Zamir D. The flowering gene SINGLE FLOWER TRUSS drives heterosis for yield in tomato. *Nat Genet*. 2010;42:459–63. <https://doi.org/10.1038/ng.550>.
- Huang X, Yang S, Gong J, Zhao Y, Feng Q, Gong H, et al. Genomic analysis of hybrid rice varieties reveals numerous superior alleles that contribute to heterosis. *Nat Commun*. 2015;6:6258. <https://doi.org/10.1038/ncomms7258>.
- Mo Z, Pu Y, Zhou J, Tian Z, Teng J, Chen Q, et al. Effect of the over-dominant expression of proteins on nicotine heterosis via proteomic analysis. *Sci Rep*. 2021;11:1–12. <https://doi.org/10.1038/s41598-021-00614-x>.
- Zhao Y, Hu F, Zhang X, Wei Q, Dong J, Bo C, et al. Comparative transcriptome analysis reveals important roles of nonadditive genes in maize hybrid An'nong 591 under heat stress. *BMC Plant Biol*. 2019;19:1–17. <https://doi.org/10.1186/s12870-019-1878-8>.
- Institutes S, Maize N, Agricultural N. Genome-wide identification and analysis of heterotic loci in three maize hybrids. 2019;6–8. <https://doi.org/10.1111/pbi.13186>.
- Shahzad K, Zhang X, Guo L, Qi T, Bao L, Zhang M, et al. Comparative transcriptome analysis between inbred and hybrids reveals molecular insights into yield heterosis of upland cotton. *BMC Plant Biol*. 2020;20:1–18. <https://doi.org/10.1186/s12870-020-02442-z>.
- Howlader J, Robin AHK, Natarajan S, Biswas MK, Sumi KR, Song CY, et al. Transcriptome Analysis by RNA-Seq Reveals Genes Related to Plant Height in Two Sets of Parent-hybrid Combinations in Easter lily (*Lilium longiflorum*). *Sci Rep*. 2020;10:1–15. <https://doi.org/10.1038/s41598-020-65909-x>.
- Qu JB, Yan KY, Li XB, Li RX, Wu SW, Cao ST. Determination of stem content in Henan tobacco leaves according to the national standard of flue-cured tobacco (grade 40). *J Chem Inf Model*. 1997;16:8–9. <https://doi.org/10.16135/j.issn1002-0861.1997.02.004>.
- Wang W, Wang Y, Yang L, Liu B, Lan M, Sun W. Studies on thermal behavior of reconstituted tobacco sheet. *Thermochim Acta*. 2005;437:7–11. <https://doi.org/10.1016/j.tca.2005.06.002>.
- Sung YJ, Seo YB. Thermogravimetric study on stem biomass of *Nicotiana tabacum*. *Thermochim Acta*. 2009;486:1–4. <https://doi.org/10.1016/j.tca.2008.12.010>.
- Zhou J, Wang J, Yu Q, Mo Z, Pu Y, Liu R. Combining ability and heterosis performance of tobacco stem percentage. *J Hunan Agric Univ Sci*. 2019;45:583–7. <https://doi.org/10.13331/j.cnki.jhau.2019.06.004>.
- Zhou JH. Analysis of Heterosis and gene differential expression of tobacco leaf stem percentage. 2020;1–52. <https://doi.org/10.27047/d.cnki.ggudu.2020.001240>.
- Murad L, Yoong Lim K, Christopodoulou V, Matyasek R, Lichtenstein CP, Kovarik A, et al. The origin of tobacco's T genome is traced to a particular lineage within *Nicotiana tomentosiformis* (Solanaceae). *Am J Bot*. 2002;89:921–8. <https://doi.org/10.2307/4131384>.

34. Sierro N, Battey JND, Ouadi S, Bakaher N, Bovet L, Willig A, et al. The tobacco genome sequence and its comparison with those of tomato and potato. *Nat Commun.* 2014;5:1–9. <https://doi.org/10.1038/ncomm54833>.
35. Song Z, Wang D, Gao Y, Li C, Jiang H, Zhu X, et al. Changes of lignin biosynthesis in tobacco leaves during maturation. *Funct Plant Biol.* 2020;48(6):624–33. <https://doi.org/10.1071/FP20244>.
36. Zou J, Li X, Dai F, Zan J, Huang Y, Wang G, et al. Comprehensive Evaluation of Tobacco-growing Soil Fertility in Karst Mountain Area — Take Xixiu District of Anshun As an Example. *J Mountain Agric Biol.* 2021;40:29–35. <https://doi.org/10.15958/j.cnki.sdnyswx.2021.02.005>.
37. Sifola M, Carrino L, Cozzolino E, Del Piano L, Graziani G, Ritieni A. Potential of pre-harvest wastes of tobacco (*Nicotiana tabacum* L.) crops, grown for smoke products, as source of bioactive compounds (phenols and flavonoids). *Sustain.* 2021;13:1–13. <https://doi.org/10.3390/su13042087>.
38. Xiang X, Wu X, Chao J, Yang M, Yang F, Chen G, et al. Genome-wide identification and expression analysis of the WRKY gene family in common tobacco (*Nicotiana tabacum* L.). *Yi Chuan.* 2016;38:840–56. <https://doi.org/10.16288/jyczz.16-016>.
39. Evans DA, Flick CE, Kut SA, Reed SM. Comparison of *Nicotiana tabacum* and *Nicotiana glauca* hybrids produced by ovule culture and protoplast fusion. *Theor Appl Genet.* 1982;62:193–8. <https://doi.org/10.1007/BF00276236>.
40. Xu JC, Zhu J. An approach for predicting heterosis based on an additive, dominance and additive x additive model with environment interaction. *Heredity (Edinb).* 1999;82:510–7. <https://doi.org/10.1038/sj.hdy.6884800>.
41. Wang S, Wu B, Xu L, Fu X, Jia X. Present situation and outlook of the utilization of flue-cured tobacco heterosis in China. *Chinese Tob Sci.* 2005;26:6–9. <https://doi.org/10.13496/j.issn.1007-5119.2005.01.002>.
42. Wang Y. Development thinking of tobacco breeding research in China. *Chinese Tob Sci.* 2001;22:2176–81. <https://doi.org/10.13496/j.issn.1007-5119.2001.04.001>.
43. Pi K, Luo W, Mo Z, Duan L, Ke Y, Wang P, et al. Overdominant expression of related genes of ion homeostasis improves K⁺ content advantage in hybrid tobacco leaves. *BMC Plant Biol.* 2022;22:1–11. <https://doi.org/10.1186/s12870-022-03719-1>.
44. Pi K, Huang Y, Luo W, Zeng S, Mo Z, Duan L, et al. Overdominant expression of genes plays a key role in root growth of tobacco hybrids. *Front Plant Sci.* 2023;14:1–13. <https://doi.org/10.3389/fpls.2023.1107550>.
45. Meng Jun. Gene differential expression analysis of tobacco upper leaf area related traits. 2018.
46. Teng J, Yu Q, Xiong J, Mo Z, Ke Y, Chen Q, et al. Expression of leaf number heterosis and differential expression of related genes in tobacco. *J South Agric.* 2021;52:420–8. <https://doi.org/10.3969/j.issn.2095-1191.2021.02.018>.
47. Mo Z, Pu Y, Zhou J, Tian Z, Teng J, Chen Q, et al. Effect of the over-dominant expression of proteins on nicotine heterosis via proteomic analysis. *Sci Rep.* 2021;11:1–12. <https://doi.org/10.1038/s41598-021-00614-x>.
48. Yoo MJ, Szadkowski E, Wendel JF. Homoeolog expression bias and expression level dominance in allopolyploid cotton. *Heredity (Edinb).* 2013;110:171–80. <https://doi.org/10.1038/hdy.2012.94>.
49. Liu H, Wang Q, Chen M, Ding Y, Yang X, Liu J, et al. Genome-wide identification and analysis of heterotic loci in three maize hybrids. *Plant Biotechnol J.* 2020;18:185–94. <https://doi.org/10.1111/pbi.13186>.
50. Liu J, Li M, Zhang Q, Wei X, Huang X. Exploring the molecular basis of heterosis for plant breeding. *J Integr Plant Biol.* 2020;62:287–98. <https://doi.org/10.1111/jipb.12804>.
51. Liu YJ, Gao SQ, Tang YM, Gong J, Zhang X, Wang YB, et al. Transcriptome analysis of wheat seedling and spike tissues in the hybrid Jingmai 8 uncovered genes involved in heterosis. *Plant.* 2018;247:1307–21. <https://doi.org/10.1007/s00425-018-2848-3>.
52. Shahzad K, Zhang X, Guo L, Qi T, Tang H, Zhang M, et al. Comparative transcriptome analysis of inbred lines and contrasting hybrids reveals overdominance mediate early biomass vigor in hybrid cotton. *BMC Genomics.* 2020;21:1–16. <https://doi.org/10.1186/s12864-020-6561-9>.
53. Botet R, Keurentjes JJB. The Role of Transcriptional Regulation in Hybrid Vigor. *Front Plant Sci.* 2020;11:1–9. <https://doi.org/10.3389/fpls.2020.00410>.
54. Luo Z, Qian J, Chen S, Li L. Dynamic patterns of circular and linear RNAs in maize hybrid and parental lines. *Theor Appl Genet.* 2020;133:593–604. <https://doi.org/10.1007/s00122-019-03489-9>.
55. Li M, Wang R, Wu X, Wang J. Homoeolog expression bias and expression level dominance (ELD) in four tissues of natural allotetraploid *Brassica napus*. *BMC Genomics.* 2020;21:1–15. <https://doi.org/10.1186/s12864-020-6747-1>.
56. Wang Z, Gerstein M, Snyder M. RNA-Seq: a revolutionary tool for transcriptomics. *Nat Rev Genet.* 2009;10:57–63. <https://doi.org/10.1038/nrg2484>.
57. Palareti G, Legnani C, Cosmi B, Antonucci E, Erba N, Poli D, et al. Metabolomics as a Driver in Advancing Precision Medicine in Sepsis. *Int J Lab Hematol.* 2016;38:42–9. <https://doi.org/10.1111/ijlh.12426>.
58. Komatsu S. Plant proteomic research 20: Trends and perspectives. *Int J Mol Sci.* 2019;20(10):2495. <https://doi.org/10.3390/ijms20102495>.
59. Tian M, Nie Q, Li ZH, Zhang J, Liu YL, Long Y, et al. Transcriptomic analysis reveals overdominance playing a critical role in nicotine heterosis in *Nicotiana tabacum* L. *BMC Plant Biol.* 2018;18:1–10. <https://doi.org/10.1186/s12870-018-1257-x>.
60. Yu Y, Zhu M, Cui Y, Liu Y, Li Z, Jiang N, et al. Genome sequence and QTL analyses using backcross recombinant inbred lines (BILs) and BILF1 lines uncover multiple heterosis-related loci. *Int J Mol Sci.* 2020;21(3):780. <https://doi.org/10.3390/ijms21030780>.
61. Shen Y, Sun S, Hua S, Shen E, Ye CY, Cai D, et al. Analysis of transcriptional and epigenetic changes in hybrid vigor of allopolyploid *Brassica napus* uncovers key roles for small RNAs. *Plant J.* 2017;91:874–93. <https://doi.org/10.1111/tpj.13605>.
62. Chaabouni S, Jones B, Delalande C, Wang H, Li Z, Mila I, et al. SH-IAA3, a tomato Aux/IAA at the crossroads of auxin and ethylene signalling involved in differential growth. *J Exp Bot.* 2009;60:1349–62. <https://doi.org/10.1093/jxb/erp009>.
63. Borovsky D, Kim Y, Hoffmann KH. Editorial: the role of peptide hormones in insect physiology, biochemistry, and molecular biology processes. *Front Physiol.* 2021;12:1–2. <https://doi.org/10.3389/fphys.2021.644907>.
64. Junli H, Shugang C, Liang J, Guixue W. Molecular mechanism of plant leaf vein development. *Chinese Bull Life Sci.* 2011;23:804–11. <https://doi.org/10.13376/j.cbils/2011.08.015>.
65. Huang J, Che S, Jin L, Qin F, Wang G, Ma N. The physiological mechanism of a drooping leaf2 mutation in rice. *Plant Sci.* 2011;180:757–65. <https://doi.org/10.1016/j.plantsci.2011.03.001>.
66. Mazzucato A, Cellini F, Bouzayen M, Zouine M, Mila I, Minoia S, et al. A TILLING allele of the tomato Aux/IAA9 gene offers new insights into fruit set mechanisms and perspectives for breeding seedless tomatoes. *Mol Breed.* 2015;35:1–5. <https://doi.org/10.1007/s11032-015-0222-8>.
67. Feng K, Hou XL, Xing GM, Liu JX, Duan AQ, Xu ZS, et al. Advances in AP2/ERF super-family transcription factors in plant. *Crit Rev Biotechnol.* 2020;40:750–76. <https://doi.org/10.1080/07388551.2020.1768509>.
68. Tsubasa SJ, Yuan L. ERF gene clusters: working together to regulate metabolism. *Trends Plant Sci.* 2021;26:23–32. <https://doi.org/10.1016/j.tplants.2020.07.015>.
69. Sakuma Y, Liu Q, Dubouzet JG, Abe H, Yamaguchi-Shinozaki K, Shinozaki K. DNA-binding specificity of the ERF/AP2 domain of Arabidopsis DREBs, transcription factors involved in dehydration- and cold-inducible gene expression. *Biochem Biophys Res Commun.* 2002;290:998–1009. <https://doi.org/10.1006/bbrc.2001.6299>.
70. Jiang F, Guo M, Yang F, Duncan K, Jackson D, Rafalski A, et al. Mutations in an AP2 transcription factor-like gene affect internode length and leaf shape in maize. *PLoS One.* 2012;7(5):e37040. <https://doi.org/10.1371/journal.pone.0037040>.
71. Salazar-Cerezo S, Martínez-Montiel N, García-Sánchez J, Pérez-y-Terrón R, Martínez-Contreras RD. Gibberellin biosynthesis and metabolism: A convergent route for plants, fungi and bacteria. *Microbiol Res.* 2018;208:85–98. <https://doi.org/10.1016/j.micres.2018.01.010>.
72. Sun T. Gibberellin Metabolism, Perception and Signaling Pathways in Arabidopsis. *Arab B.* 2008;6:e0103. <https://doi.org/10.1199/tab.0103>.
73. He J, Xin P, Ma X, Chu J, Wang G. Gibberellin metabolism in flowering plants: an update and perspectives. *Front Plant Sci.* 2020;11:5–10. <https://doi.org/10.3389/fpls.2020.00532>.
74. Li J, Gao H, Wang Z, Jiang J, Dzyubenko N, Chapurin V, et al. Overexpression of the *Galega orientalis* gibberellin receptor improves biomass

- production in transgenic tobacco. *Plant Physiol Biochem.* 2013;73:1–6. <https://doi.org/10.1016/j.plaphy.2013.07.015>.
75. Gao LW, Lyu SW, Tang J, Zhou DY, Bonnema G, Xiao D, et al. Genome-wide analysis of auxin transport genes identifies the hormone responsive patterns associated with leafy head formation in Chinese cabbage. *Sci Rep.* October 2016;2017(7):1–13. <https://doi.org/10.1038/srep42229>.
 76. Li X, Wu P, Lu Y, Guo S, Zhong Z, Shen R, et al. Synergistic interaction of phytohormones in determining leaf angle in crops. *Int J Mol Sci.* 2020;21:1–18. <https://doi.org/10.3390/ijms21145052>.
 77. Mu X, Chen Q, Wu X, Chen F, Yuan L, Mi G. Gibberellins synthesis is involved in the reduction of cell flux and elemental growth rate in maize leaf under low nitrogen supply. *Environ Exp Bot.* 2018;150:198–208. <https://doi.org/10.1016/j.envexpbot.2018.03.012>.
 78. Chen M, Maodzeka A, Zhou L, Ali E, Wang Z, Jiang L. Removal of DELLA repression promotes leaf senescence in Arabidopsis. *Plant Sci.* 2014;219–220:26–34. <https://doi.org/10.1016/j.plantsci.2013.11.016>.
 79. Ritonga FN, Zhou D, Zhang Y, Song R, Li C, Li J, et al. The roles of gibberellins in regulating leaf development. *Plants.* 2023;12:1–19. <https://doi.org/10.3390/plants12061243>.
 80. Xuan Y, Zhao HF, Guo XY, Ren J, Wang Y, Lu BY. Plant cell wall remodeling enzyme xyloglucan endotransglucosylase/hydrolase (XTH). *Chin Agri Sci Bull.* 2016;32:83–8.
 81. Cosgrove DJ. Growth of the plant cell wall. *Nat Rev Mol Cell Biol.* 2005;6:850–61. <https://doi.org/10.1038/nrm1746>.
 82. Matsui A, Yokoyama R, Seki M, Ito T, Shinozaki K, Takahashi T, et al. AtXTH27 plays an essential role in cell wall modification during the development of tracheary elements. *Plant J.* 2005;42:525–34. <https://doi.org/10.1111/j.1365-313X.2005.02395.x>.
 83. Zhang B, Liu J, Yang ZE, Chen EY, Zhang CJ, Zhang XY, et al. Genome-wide analysis of GRAS transcription factor gene family in *Gossypium hirsutum* L. *BMC Genomics.* 2018;19:1–12. <https://doi.org/10.1186/s12864-018-4722-x>.
 84. Martinez-García JF, Moyano E, Alcocer MJC, Martin C. Two bZIP proteins from *Antirrhinum* flowers preferentially bind a hybrid C-box/G-box motif and help to define a new sub-family of bZIP transcription factors. *Plant J.* 1998;13:489–505. <https://doi.org/10.1046/j.1365-313X.1998.00050.x>.
 85. Bano N, Patel P, Chakrabarty D, Bag SK. Genome-wide identification, phylogeny, and expression analysis of the bHLH gene family in tobacco (*Nicotiana tabacum*). *Physiol Mol Biol Plants.* 2021;27:1747–64. <https://doi.org/10.1007/s12298-021-01042-x>.
 86. Li N. Cloning and Functional characterization of CibHLH027 involved in leaf senescence from *Caragana intermedia*. 2017.
 87. Donner TJ, Scarpella E. Auxin-transport-dependent leaf vein formation. *Botany.* 2009;87:678–84. <https://doi.org/10.1139/B09-002>.
 88. Martin C, Paz-Ares J. MYB transcription factors in plants. *Trends Genet.* 1997;13:67–73. [https://doi.org/10.1016/S0168-9525\(96\)10049-4](https://doi.org/10.1016/S0168-9525(96)10049-4).
 89. Stracke R, Holtgräwe D, Schneider J, Pucker B, Rosleff Sörensen T, Weisshaar B. Genome-wide identification and characterisation of R2R3-MYB genes in sugar beet (*Beta vulgaris*). *BMC Plant Biol.* 2014;14:1–17. <https://doi.org/10.1186/s12870-014-0249-8>.
 90. Byrne ME, Barley R, Curtis M, Arroyo JM, Dunham M, Hudson A, et al. Asymmetric leaves1 mediates leaf patterning and stem cell function in Arabidopsis. *Nature.* 2000;408:967–71. <https://doi.org/10.1038/35050091>.
 91. Lee DK, Geisler M, Springer PS. LATERAL ORGAN FUSION1 and LATERAL ORGAN FUSION2 function in lateral organ separation and axillary meristem formation in Arabidopsis. *Development.* 2009;136:2423–32. <https://doi.org/10.1242/dev.031971>.
 92. Jaradat MR, Feurtado JA, Huang D, Lu Y, Cutler AJ. Multiple roles of the transcription factor AtMYBR1/AtMYB44 in ABA signaling, stress responses, and leaf senescence. *BMC Plant Biol.* 2013;13:192. <https://doi.org/10.1186/1471-2229-13-192>.
 93. Guo Y, Gan S. AtMYB2 regulates whole plant senescence by inhibiting cytokinin-mediated branching at late stages of development in Arabidopsis. *Plant Physiol.* 2011;156:1612–9. <https://doi.org/10.1104/pp.111.177022>.
 94. Hou H, Zhang C, Hou X. Cloning and functional analysis of bcbmyb101 gene involved in leaf development in Pak choi (*Brassica rapa* ssp. chinensis). *Int J Mol Sci.* 2020;21:1–16. <https://doi.org/10.3390/ijms21082750>.
 95. Mizutani M, Ohta D. Diversification of P450 genes during land plant evolution. *Annu Rev Plant Biol.* 2010;61:291–315. <https://doi.org/10.1146/annurev-arplant-042809-112305>.
 96. Zondlo SC, Irish VF. CYP78A5 encodes a cytochrome P450 that marks the shoot apical meristem boundary in Arabidopsis. *Plant J.* 1999;19:259–68. <https://doi.org/10.1046/j.1365-313X.1999.00523.x>.
 97. Anastasiou E, Kenz S, Gerstung M, MacLean D, Timmer J, Fleck C, et al. Control of Plant Organ Size by KLUH/CYP78A5-Dependent Intercellular Signaling. *Dev Cell.* 2007;13:843–56. <https://doi.org/10.1016/j.devcel.2007.10.001>.
 98. Wang JW, Schwab R, Czech B, Mica E, Weigel D. Dual effects of miR156-targeted SPL genes and CYP78A5/KLUH on plastochron length and organ size in Arabidopsis thaliana. *Plant Cell.* 2008;20:1231–43. <https://doi.org/10.1105/tpc.108.058180>.
 99. Zhao L, Cai H, Su Z, Wang L, Huang X, Zhang M, et al. KLU suppresses megasporocyte cell fate through SWR1-mediated activation of WRKY28 expression in Arabidopsis. *Proc Natl Acad Sci U S A.* 2018;115:E526–35. <https://doi.org/10.1073/pnas.1716054115>.
 100. Christ B, Süssenbacher I, Moser S, Bichsel N, Egert A, Müller T, et al. Cytochrome P450 CYP89A9 is involved in the formation of major chlorophyll catabolites during leaf senescence in Arabidopsis. *Plant Cell.* 2013;25:1868–80. <https://doi.org/10.1105/tpc.113.112151>.
 101. Que YH, He Y, Yu QW, Xiong J, Luo W, Wang PS, et al. Effects of different drying methods and equilibrium moisture content on tobacco stem content. *Spec Wild Anim Plant Res.* 2022;61:90–4. <https://doi.org/10.16720/j.cnki.tcyj.2022.034>.
 102. Kim D, Langmead B, Salzberg SL. HISAT: A fast spliced aligner with low memory requirements. *Nat Methods.* 2015;12:357–60. <https://doi.org/10.1038/nmeth.3317>.
 103. Pertea M, Pertea GM, Antonescu CM, Chang TC, Mendell JT, Salzberg SL. StringTie enables improved reconstruction of a transcriptome from RNA-seq reads. *Nat Biotechnol.* 2015;33:290–5. <https://doi.org/10.1038/nbt.3122>.
 104. Li B, Dewey CN. RSEM: Accurate transcript quantification from RNA-seq data with or without a reference genome. *Bioinforma Impact Accurate Quantif Proteomic Genet Anal Res.* 2011;1:1–16. <https://doi.org/10.1201/b16589>.
 105. Love MI, Huber W, Anders S. Moderated estimation of fold change and dispersion for RNA-seq data with DESeq2. *Genome Biol.* 2014;15:1–21. <https://doi.org/10.1186/s13059-014-0550-8>.
 106. Xie C, Mao X, Huang J, Ding Y, Wu J, Dong S, et al. KOBAS 2.0: a web server for annotation and identification of enriched pathways and diseases. *Nucleic Acids Res.* 2011;39(Web Server issue):316–22. <https://doi.org/10.1093/nar/gkr483>.
 107. Livak KJ, Schmittgen TD. Analysis of relative gene expression data using real-time quantitative PCR and the 2^{-ΔΔCT} method. *Methods.* 2001;25:402–8. <https://doi.org/10.1006/meth.2001.1262>.

Publisher's Note

Springer Nature remains neutral with regard to jurisdictional claims in published maps and institutional affiliations.